

IMPT plans were prescribed to deliver 67.5 Gy to the prostate and 60 Gy to the seminal vesicles over 25 fractions. In the case of IMPT, corresponding doses were prescribed as Gy(RBE). The dosimetric and volumetric distributions for each treatment plan were evaluated with respect to risk of radiation-induced cancer by using both the linear-no-threshold (LNT) model and the non-linear competitive risk model which incorporates cell killing vs induction of carcinogenic mutations in fractionated RT [Dasu et al, 2005]. The organ equivalent dose (OED) concept [Schneider et al, 2005] was adapted to both risk-response models and served as a relative risk measure, while estimates of absolute risks were based on five nominal risk calculation methods of organ-specific radiation induced cancer as suggested by the International Commission on Radiological Protection [ICRP 103, 2007].

Results: All treatment plans fulfilled the plan optimisation criteria as defined by standardised treatment protocols. The IMPT generally achieved a lower integrated dose to healthy tissues (Figure 1), and mean doses to the bladder and rectum were reduced as well as the percentage of the volumes receiving 20 Gy and 40 Gy. The linear risk models compared in favour of IMPT for both organs at risk (Table 1). The corresponding results using the competition model resulted in a 1.7 times higher risk of bladder cancer from VMAT compared to IMPT, while no significant difference was seen between the two techniques for the rectum. Translating the relative scoring from the competition model into absolute quantities, the risks for VMAT and IMPT were 0.2-0.5 % and 0.1-0.3 %, respectively. The risks of radiation induced rectal cancer were estimated to 0.1-0.3 % for both radiation modalities.

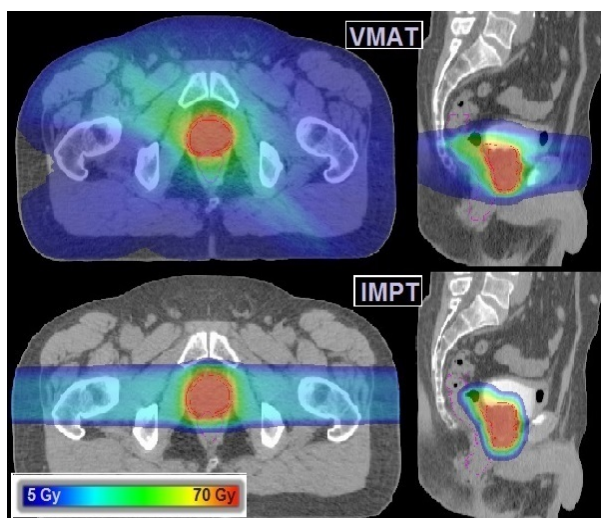


Figure 1. Dose distributions 5-70 Gy for VMAT (partial single arc with posterior avoidance sector 12°) and 5-70 Gy(RBE) proton IMPT delivered by lateral-opposing fields. Generated in the Eclipse treatment planning system [Varian Medical Systems, Palo Alto, CA, USA].

Table 1. Summary of dosimetric and volumetric parameters presented as mean (standard deviation) of ten patients including OED and risks of radiation-induced secondary cancer as predicted by linear risk model and competition model. Absolute risk estimates were based on nominal risks from different methods of calculation presented in ICRP 103. P-value of two tailed t-test.

	Index	VMAT	IMPT	P-value
Bladder	D2cc [Gy]	65.1 (1.9)	65.3 (1.8)	>0.10
	V20 [%]	52.5 (12.3)	27.0 (13.6)	<0.001
	V40 [%]	22.6 (9.1)	17.2 (10.0)	<0.001
	Dmean [Gy]	24.6 (5.8)	14.3 (7.2)	<0.001
	OEDComp [Gy]	0.47 (0.19)	0.28 (0.05)	0.03
	Risk Linear	9.9 - 24.6 %	5.7 - 14.3 %	
	Risk Comp	0.2 - 0.5 %	0.1 - 0.3 %	
Rectum	D2cc [Gy]	61.3 (2.4)	61.8 (2.3)	0.02
	V20 Gy [%]	65.5 (12.4)	31.2 (10.7)	<0.001
	V40 Gy [%]	30.2 (9.5)	20.2 (5.9)	<0.001
	Dmean [Gy]	28.8 (16.5)	16.5 (4.7)	<0.001
	OEDComp [Gy]	0.38 (0.13)	0.35 (0.05)	>0.10
	Risk Linear	5.8 - 24.0 %	3.3 - 13.8 %	
	Risk Comp	0.1 - 0.3 %	0.1 - 0.3 %	

Conclusions: When incorporating effects of non-linear dose-response and fractionated RT, VMAT resulted in 1.7 times higher risk of radiation-induced bladder cancer compared to IMPT, while no significant difference between the two techniques was found for secondary rectal cancer.

PO-0913

Machine learning-based prediction of late radiation-induced lung toxicity in Hodgkin's lymphoma survivors
 R. Pacelli¹, J.H. Oh², J.O. Deasy², M. Conson¹, V. D'Avino³, M. Picardi⁴, M.C. Pressello⁵, G. Boboc⁶, R. Battistini⁷, V. Donato⁶, L. Cella³

¹Università degli Studi di Napoli, Dipartimento di Scienze Biomediche Avanzate, Napoli, Italy

²Memorial Sloan-Kettering Cancer Center, Department of Medical Physics, New York, USA

³Consiglio Nazionale delle Ricerche, Istituto di Biostrutture e Bioimmagini, Napoli, Italy

⁴Università degli Studi di Napoli, Dipartimento di Medicina e Chirurgia, Napoli, Italy

⁵Azienda Ospedaliera San Camillo Forlanini, UOC Fisica Sanitaria, Rome, Italy

⁶Azienda Ospedaliera San Camillo Forlanini, UOC Radioterapia, Rome, Italy

⁷Azienda Ospedaliera San Camillo Forlanini, UOC Ematologia, Rome, Italy

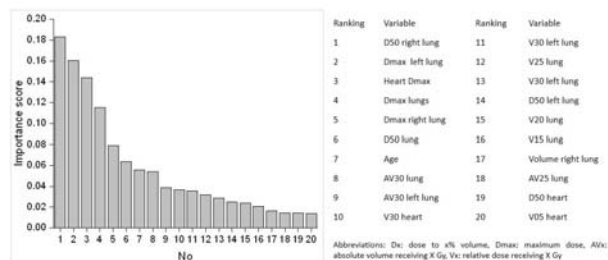
Purpose/Objective: Hodgkin's lymphoma (HL) radiation treatments may be responsible for late-phase subclinical lung radiation-induced injury such as fibrosis with radiological lung density changes detectable by computed tomography (CT). Using a machine-learning technique, our purpose was to investigate variable importance in predicting radiation-induced CT changes in HL survivors treated with chemotherapy and radiotherapy (RT). The potential role of heart irradiation on the risk of CT changes was also investigated.

Materials and Methods: One hundred ten consecutive patients treated with sequential chemo-radiotherapy for supradiaphragmatic HL (median follow-up 68 months, range 13-140) were retrospectively reviewed for radiological signs of lung CT changes. All patients were treated with three-dimensional conformal radiotherapy with a median total dose of 30.6 Gy (range 14.4-45). At a median time of 16.5 months (range 6-102), 18 of 110 patients (16.4%) developed lung

radiological changes on CT after treatment. Median patient age was 28 years (range 6-71). In addition to lung irradiation factors, clinical variables, along with left and right lung and heart dose-volume histogram parameters, were included in the analysis. We applied a random forest (RF) algorithm to assess the prediction power and to measure the importance of the variables. We split the cohort into two groups with one group (toxicity group) having lung toxicity and the other group (case group) without toxicity. To make balanced data, we randomly selected 18 samples from the case group and combined them with 18 samples in the toxicity group, resulting in 36 patients in total. With the 36 patients, we performed a two-stage of RF. In the first RF, all predictors were used, selecting 1/3 of predictors at node split. Based on the out-of-bag (OOB) samples, we calculated the importance of each variable and removed 1/3 insignificant variables for further analysis. Then, using the remaining predictors, the second RF was performed, still choosing 1/3 of predictors at each node split from the remaining predictors. This procedure was iterated 50 times. Model performance was assessed using the area under the receiver operating characteristic curve (AUC).

Results: In the first RF, AUC=0.62 was obtained on average. In the second RF, a slightly better performance was obtained with AUC=0.64 on average. RF variable importance scores for the top 20 predictors relevant to CT changes obtained in the first RF are presented in figure 1. It was observed that both lung and heart-related predictors were highly ranked, suggesting that there is a correlation between doses received in heart and CT changes in lung.

Figure 1



Conclusions: Applying RF method, we showed the importance of jointly considering lung and heart irradiation in the prediction of subclinical radiation-induced lung fibrosis. Although asymptomatic, lung fibrosis could result in future respiratory insufficiency and its prediction is important for long-term quality of life for HL survivors.

PO-0914

Knowledge-based automated VMAT Planning for liver metastases

A.W.M. Sharfo¹, M.L.P. Dirks¹, S. Breedveld¹, B.J.M. Heijmen¹, A.M. Mendez Romero¹

¹Erasmus MC-Cancer Institute, Radiation Oncology / Radiotherapy, Rotterdam, The Netherlands

Purpose/Objective: To investigate whether computer-optimized fully automated VMAT planning may improve treatment plans for patients with liver metastases.

Materials and Methods: Nine patients with liver metastases, previously treated in our clinic at a Cyberknife (CK) to 60 Gy

prescribed at the 80% isodose, were included in this study. For each study patient, using our in-house developed multi-criterial optimizer for fully automated plan generation, an optimized plan with 29 equidistant coplanar beams was generated. Our optimizer uses the 2-phase ϵ -constraint (2pec) lexicographic optimization algorithm, based on a fixed list of hard constraints and prioritized objectives. This so-called 'wish-list' is generated in an iterative procedure based on physicians' evaluation of initial plans generated for the first few patients. First priority was to achieve the highest possible coverage of the planning target volume (PTV) by the prescription dose, while not violating the clinically applied hard constraints. After optimization, a template containing the achieved results for the objectives and constraints is automatically generated, and fed into the clinical TPS (Monaco 5.0) to generate a clinically deliverable dual-arc VMAT plan without requiring any human interference. This plan was compared to the manually generated CK plan, comprising multiple non-coplanar beams, with respect to PTV dose coverage, mean dose and near-maximum dose ($D_{2\%}$) in the OARs.

Results: In the automatically generated VMAT plans, PTV coverage increased by 0.8% on average ($p = 0.594$). All VMAT plans complied with the clinical constraints. This also applied to the patients in which the maximum dose in the spinal cord was slightly, but not significantly higher than in the CK plans ($p = 0.314$). For most of the other OARs large reductions in mean and near-maximum doses were observed (see Figure). The volumes of healthy liver receiving 15 Gy, 18 Gy and 21.6 Gy (clinical constraints) were reduced by 1%, 3.7% and 1.6%, respectively. In addition the mean dose in the healthy liver was significantly reduced by 2.5 ± 0.8 Gy ($p = 0.008$). The near-maximum dose in the bowel, duodenum, esophagus, heart, right kidney and gallbladder was significantly lower ($p < 0.05$), with population mean reductions of 20.7%, 22.5%, 11.9%, 27.4%, 18.8% and 20.6%, respectively. Estimated delivery times for VMAT were a factor of eight shorter compared to CK plans (5.3 ± 1.3 minutes versus 42 ± 12 minutes).

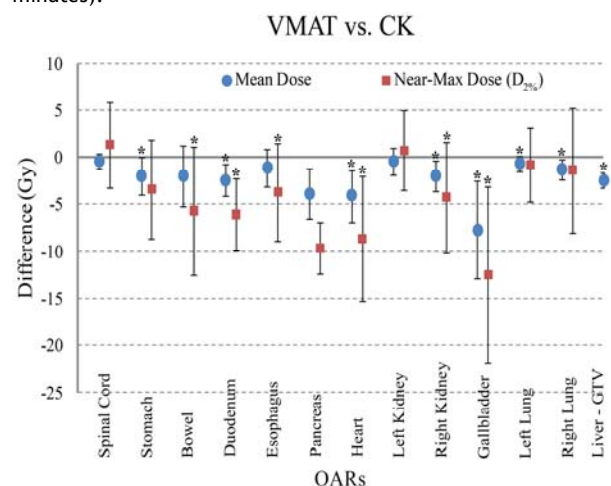


Figure: Difference in OARs near-maximum and mean doses for automatically generated VMAT plans compared to CK plans. The dots give the population mean values for the 9 study patients and the error bars indicate ± 1 standard deviation.